INTRODUCTION

Micronutrient deficiencies affect a large proportion of the world population (www.who.int). Iron deficiency is the most widespread nutritional disorder worldwide and has a negative impact on health, lifespan, and productivity. Zinc deficiency results in increased risk of malaria, diarrhea, and pneumonia, and is estimated to be responsible for 4.4% of mortality in children under 5 years of age [1].

Micronutrient deficiencies affect primarily children and pregnant women in low-income, vulnerable populations, whose diets often rely on a few starchy staple crops. Biofortification by the breeding of staples with increased micronutrient content is a sustainable approach to reduce micronutrient malnutrition in these populations [2,3,4,5]. Legumes are micronutrient-rich, and iron biofortification of common beans is expected to decrease the iron deficiency burden by 9% to 33% in Northern Brazil [2,6,7].

Soy products including soy flour, soy protein, and soy milk substitute, are used in food assistance programs to improve the diet in developing countries (www.ific.org, www.wishh.org). These products provide protein and calories and can provide important micronutrients. It has been shown that soybeans (*Glycine max*) are a good source of nutritional iron [8].

Micronutrient content, localization, and speciation affect bioavailability. Between 70% and 95% of the seed iron in common beans and soybeans accumulates in the cotyledons, but iron distribution is dependent on genotype [9],[10,11]. In the model plant, *Arabidopsis thaliana*, iron, zinc, and manganese were shown to accumulate in distinct regions within the mature seed cotyledon and radicle [12]. Furthermore, iron distribution within the seed was affected by the disruption of the vacuolar iron uptake transporter VIT1 [12].

To our knowledge, the detailed distribution of micronutrients within the mature soybean seed has not previously been described. In this study we used the sensitive, non-destructive micro-PIXE (Particle Induced X-ray Emission) technique to determine the distribution of nutritionally important elements within soybean seeds. In addition, we used the Perl's Prussian blue technique to study the cellular localization of iron within the soybean seed coat and radicle.

MATERIALS AND METHODS

Plant materials. We used soybeans purchased at retailers in South Africa (*G. max* 1) and in Denmark (*G. max.* 2), soybean genotypes Caloria (*G. max* 3) and Wayne (*G. max* 4), *P. coccineus* beans purchased at a retailer in Denmark, and three *Phaseolus vulgaris* genotypes, NUA 35, G19833, and G14519 obtained from the International Center for Tropical Agriculture, Cali, Colombia.

Average concentrations of elements in different tissues of soybeans. For each genotype, ten to twenty dry mature seeds were dissected into embryo axis, cotyledons, and seed coat tissues using a razor blade. Fe, Mn, and Zn content of each tissue was measured in duplicates at the Institute of Technology, Kongsvang Alle 29, 8000 Aarhus C, Denmark, using inductively coupled plasma atomic emission spectroscopy (ICP-AES) in axial mode.

Micro-PIXE analysis. Both dry and soaked soybean seeds were cut with a razor blade. Air-dried samples were mounted on a thin Formvar layer. After coating the seed surfaces with carbon, microanalyses were performed using the nuclear microprobe at the Materials Research Group, iThemba LABS, South Africa. A proton beam of 3.0 MeV energy and 100-150 pA current was focused to a 3 x 3 μm^2 spot and raster scanned over the areas of interest, using square or rectangular scan patterns with a variable number of pixels (up to 128 x 128). Particle-induced X-

ray emission (PIXE) and proton backscattering spectrometry (BS) were used simultaneously as previously described [13,14,15]. Elemental concentrations were obtained using GeoPIXE II software [16]. Quantitative elemental images were generated using the *Dynamic Analysis* method. Information on atomic ratios of light elements forming organic matrix, necessary for PIXE quantitative analysis, was found from BS technique. PIXE and BS spectra were extracted from selected regions of the analyzed tissue to obtain the average concentrations of the analyzed elements within them.

Colorimetric detection of iron in seed samples. Perl's Prussian Blue (PPB) method was used as previously described [17],[18].

Preparation of samples for light microscopy. Samples stained with PPB method as previously described were incubated overnight in 70% ethanol prior to fixation. The tissue was thereafter fixed for 24 to 48 hours at 4°C in 4% paraformaldehyde, 1% glutaraldehyde, 0.1M $NaHPO_4$ pH 7.2. A stepwise dehydration in ethanol was performed using 30 min incubations in 70%, 80%, 90%, and twice in 96% ethanol. For embedding and polymerization we used the Technovit 7100 kit (Heraeus Kulzer, Wehrheim, Germany). Embedding was performed using stepwise increments of Technovit hardener I in ethanol, and manufacturers' recommendations were followed for the polymerization. The specimens were sectioned into 7-11 micrometer thick samples using a Leica RM2045 microtome and studied by light microscopy.

RESULTS:

Soybean seed coats contain high concentrations of iron, while the embryonic axis is rich in zinc and iron. It has previously been shown that the levels of important micronutrients such as iron, zinc, and manganese in the seed coats and embryo of soybean seeds vary with their developmental stages [11]. In this study we divided the mature soybean embryo into the cotyledons and the embryonic axes prior to ICP-AES analyses. The concentrations of iron, zinc and manganese in the cotyledons, embryonic axes, and seed coats of four soybean genotypes are shown in Table 1. The highest iron concentrations were measured in the seed coats (230 to 410 ppm), while the lowest were found in the cotyledons (38-64 ppm) (Table 1). For zinc, the highest concentrations were found in the embryonic axis and ranged from 57 to 140 ppm. In comparison, the cotyledons contained 34 to 61 ppm of zinc. The concentration of manganese in the cotyledon was similar to the concentration in the embryonic axis, at 23 to 34 ppm, while seed coat manganese ranged from 12 to 17 ppm.

G. max	**1**				**2**				**3**				**4**			
Element	Fe	Mn	Zn	%dw	Fe	Mn	Zn	%dw	Fe	Mn	Zn	%dw	Fe	Mn	Zn	%dw
E. axis	100	30	62	2.3	95	23	57	2.6	97	31	95	3.1	120	34	140	2.9
Cotyledon	38	ND	35	7.3	43	23	34	6.7	64*	34	61	7.9	50	31	54	7.2
Seed coat	410	17	33	90	390	12	26	90	250	13	62	90	230	ND	96	90

Table 1: Iron, manganese, and zinc concentrations in different tissues of mature soybeans*. The concentration of iron (Fe), manganese (Mn), and zinc (Zn) in seed coats, embryonic axis (E. axis), and cotyledons was determined using ICP-AES in axial mode. Unless otherwise stated, all values are average of at least two measurements and are given in micrograms/gram dry mass (ppm). The relative standard deviations (%RSD) are 10 for iron, 9.7 for manganese, and 8.1 for zinc. The average dry weight of each tissue, as a percentage of the total seed dry weight is shown (%dw). *: single measurement, ND: not determined.*

Elemental distribution within individual tissues of soybean seeds. To study whether this was the case in soybean seeds, we used the micro-PIXE technique. It was clear that high concentrations of both iron and manganese accumulate at or near the provascular bundles of the

un-soaked soybean radicle (Fig. 1B and E). In agreement with the ICP-AES measurements, the highest concentrations of iron were observed in the seed coat. Seed coat regions (Fig. 1 B, G, and H regions 5-6) accumulated more than 600 ppm of iron, while the hilum contained less than 100 ppm of iron (Fig. 1 G-H, region 4).

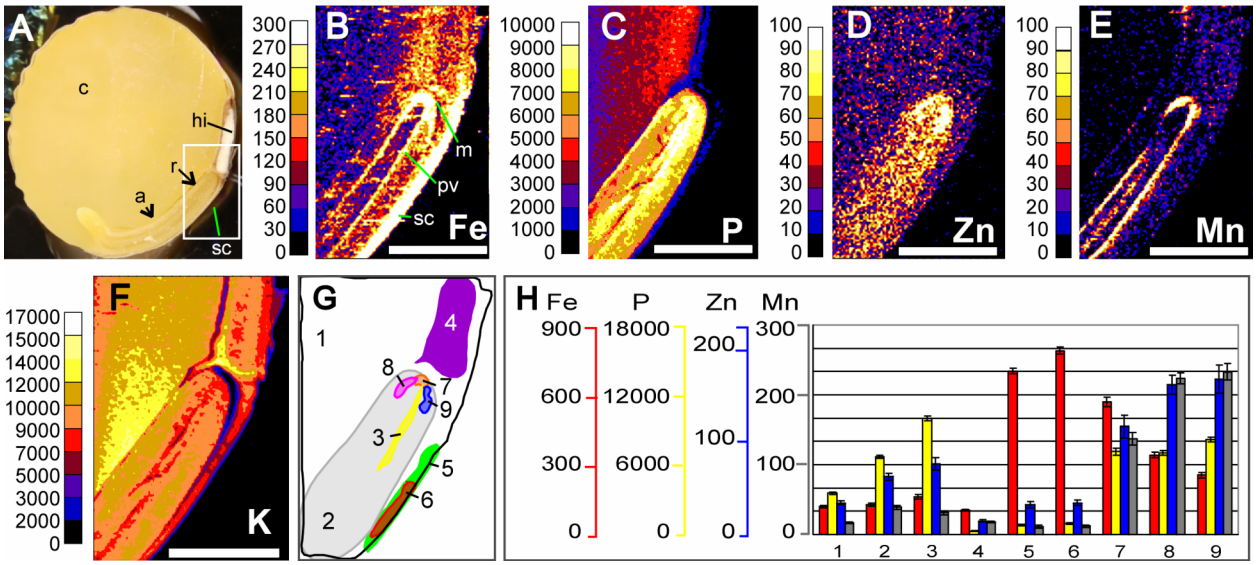

Fig. 1 Elemental analysis of mature soybean using micro-PIXE. *Elemental maps obtained by Dynamic Analysis method. Maps of iron (B), phosphorus (C), zinc (D), manganese (E), and potassium (F) distribution in a section of G. max1 (A). The scanned area is marked with an open square in A. Color scales on the left side of each map show concentrations in micrograms/gram dry mass . Scale bars are 1 mm. The average concentrations of elements from areas illustrated in G are shown in the bar chart (H). The concentrations of iron, phosphorus, zinc, and manganese are shown in red, yellow, blue, and grey, respectively. All values are in micrograms/gram dry tissue. a: embryo axis, m: meristem, sc: seed coat, pv: provascular tissue, r: radicle, c: cotyledon, and hi: hilum.*

To test whether elements are redistributed by soaking, the soybean seeds were soaked in water for 10 hours prior to hand sectioning, drying, and micro-PIXE analysis. Seed coat iron is remarkably lower in the soaked seed coat compared to the un-soaked tissue. This is illustrated in Fig. 2 and Table 2. While the seed coat from the un-soaked soybean contained 588 ppm of iron (Fig. 2G region 5), soaked soybean contained 117 and 125 ppm of this element (Fig. 2B regions 1 and 2).

The radicle meristem of the unsoaked soybeans had the highest concentrations of manganese and zinc, and 200-600 ppm of iron (Fig. 1G-H, regions 7-8). The radicles are also rich in phosphorus, but more potassium accumulates in the cotyledon than in the radicle (Fig. 1C and F). To achieve a more detailed picture of the distribution of manganese and iron in the radicle tip, we performed an angled cross section of this tissue and analyzed it using micro-PIXE (Fig. 2H-J). Iron is accumulated in or near the provascular tissue of the radicle, while manganese accumulates in a pattern similar to that of iron and in the center of the procambium (pc) (Fig. 1E and Fig. 2I). This region has an average of 86 ppm of manganese which is seven times higher than the average concentration of manganese in the analyzed radicle tissue (Fig. 2I and Table 2, region 8 compared to Total H-J). The iron concentration in the procambium region (region 8) is lower than the average of iron in the analyzed sample.

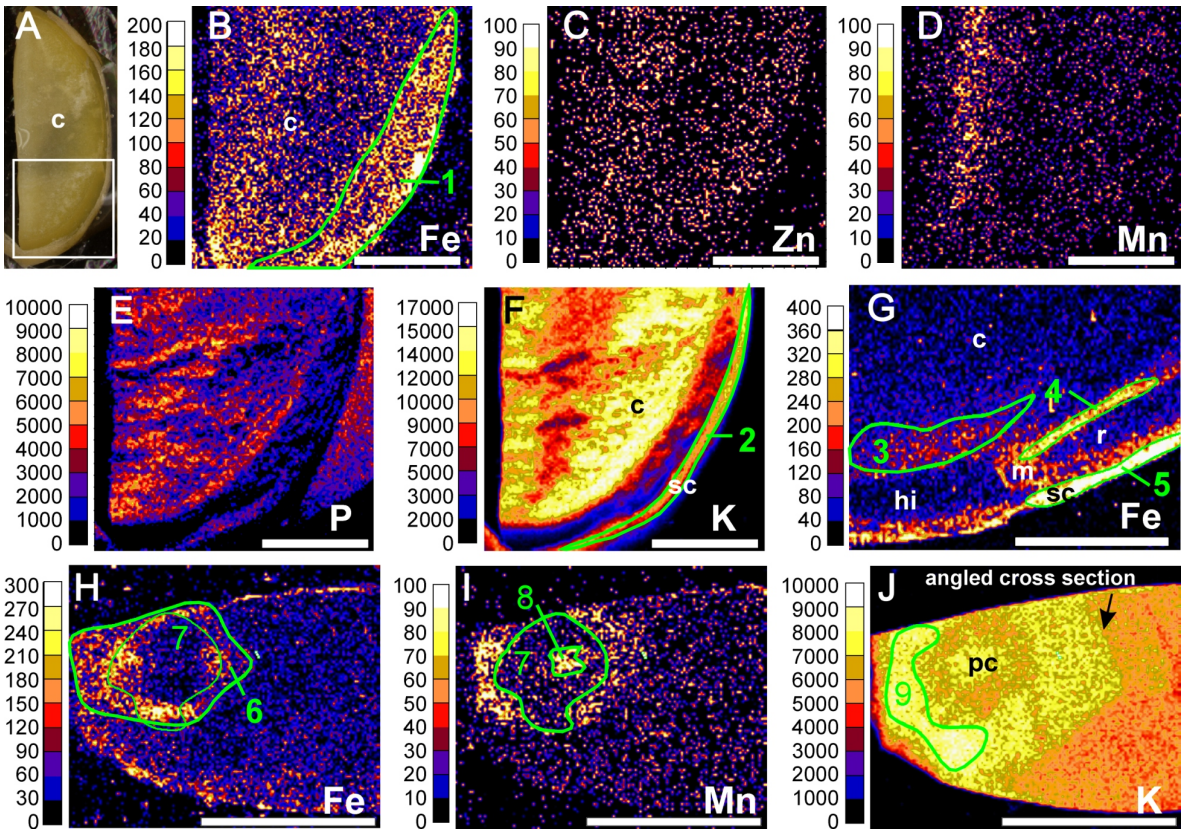

Fig. 2 Micro-PIXE elemental analysis of different tissues of the soybean G. max 2. *Maps of iron (B), zinc (C), manganese (D), phosphorus (E), and potassium (F) distribution in a section of a cotyledon (shown in A) from G. max 2 that have been soaked in water for 10 hours. The scanned area is marked with an open square in A. The iron map of unsoaked tissue of G. max 2 is shown in G. Close up analysis of a radicle from an unsoaked soybean seed (G. max 2) with an angle cross section at the radicle tip. The iron (H), manganese (I), and potassium (J) maps are shown. Color scales on the left side of each map show concentrations in micrograms/gram dry mass. Scale bars are 1 mm. The average concentrations of elements from areas marked with green outlines are shown in Table 2. m: meristem, sc: seed coat, r: radicle, c: cotyledon, hi: hilum, and pc: procambium.*

Region	**P**	**K**	**Mn**	**Fe**	**Zn**
Total B-F	2275±110	10050±90	12±1	70±3	28±2
1	1230±80	10840±155	< 4	125±5	27±3
2	1020±95	7080±110	5±1	117±4	33±2
Total G	2900±75	11500±80	20±2	114±8	41±3
3	4560±130	14490±270	32±3	139±6	54±2
4	6950±130	8910±170	99±4	310±9	116±6
5	415±40	11320±200	10±3	588±11	14±3
Total H-J	5220±90	8210±45	12±1	77±5	67±6
6	7475±115	8980±60	30±2	119±5	100±6
7	7315±115	9390±70	49±3	121±6	115±5
8	7610±130	9715±50	86±9	57±7	78±11
9	8505±110	10370±70	37±2	113±4	138±7

Table 2. Elemental concentration in regions of soybean tissues*. The regions correspond to the areas outlined in green in Fig. 2 and the values are given n micrograms/gram dry mass (ppm). The average elemental concentration in the analyzed sample are also shown (Total B-F, G, and H-J, respectively). < 4: below detection limit*

Cellular distribution of iron in soybeans. The Perl's Prussian blue method was used to study the cellular localization of iron in soybeans. Whole soybeans were soaked in water for 18 hours prior to hand sectioning and Perl's Prussian blue staining. Intense blue stain was observed in the seed coat tissues, indicating that even after soaking, iron is present in the seed coats (Fig. 3A). Iron stain was also detected near the epidermal cells of the cotyledons and in the radicle. In agreement with the micro-PIXE analysis, microscope pictures of the radicle showed blue staining of the provascular cells (Fig. 3B and C). Sections of seed coat tissue stained using the Perl's Prussian blue method showed that iron was present in different cell types of the seed coats. In particular, a layer of blue color was observed near the hilum between the palisade (pl) and counter palisade (cp) cell layers (Fig. 3F and G). In addition some compressed parenchyma cells (pa) showed blue staining (Fig. 3H and I) and in some cases blue color was clearly localized to the palisade (pl) cells as illustrated in Fig. 3J. The stain patterns in Fig. 3H and I, indicate the occurrence of re-distribution of the stained iron, in agreement with the previous results indicating a reduction of iron content in the seed coats after soaking.

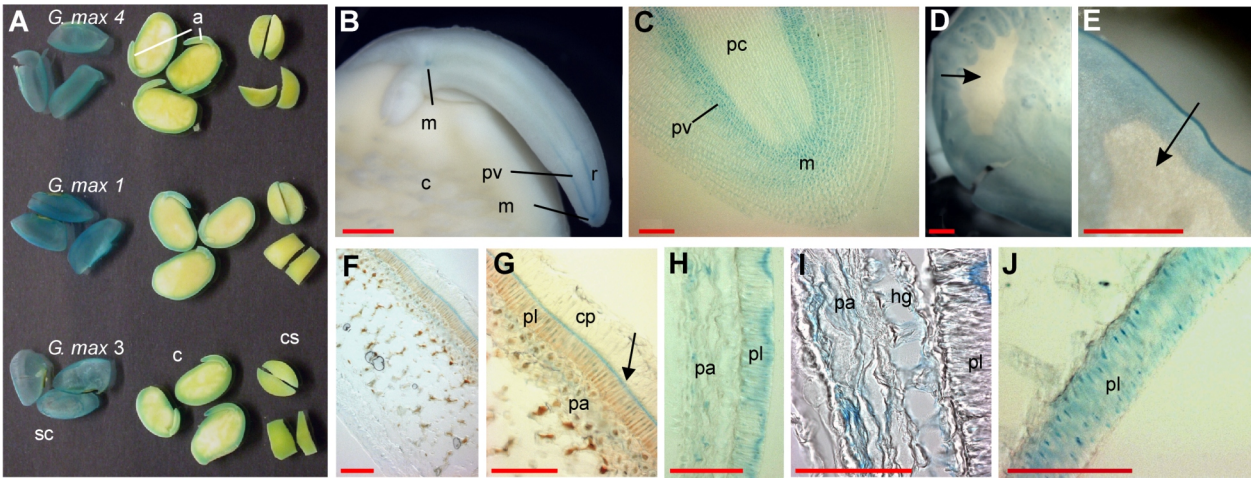

Fig. 3 Perl's blue staining of mature soybean seeds*. D-E: non-soaked seeds stained with Perl's solution for 20 min. A-C and F-J: the seeds were soaked in water for 18 hours prior to staining. A: stained seed coats (sc) and cotyledons (c) of G. max 1, 3, and 4. B-C: close-up of the embryo axis showing strong staining of the shoot and root meristems (m) and of the provascular tissue (pv) of the radicle (r). C: enlarged picture of the radicle. D-E: stereomicroscope captures of stained seed coat from non-soaked soybeans, showing a patch where the seed coat did not detach from the cotyledons (arrows) and therefore was not stained by the Perl's solution. F-J: light microscopy pictures of seed coat sections. F: section of seed coat near the hilum, G: enlargement of F showing the palisade layer (pl) and the counter palisade layer (cp). Iron is accumulated between these two layers (arrow). H, J: seed coat sections showing iron stain of the palisade layer (pl) and the parenchyma cells (pa). I: enlargement of H. The scale bars are 1 mm in B, D and E, and 0.1 mm in C, and in F to J. a: embryo axis, cs: cross section, pc: procambium, pl: palisade layer, cp: counter palisade layer, pa: parenchyma cells, hg: hourglass cells.*

Our results also indicate that seed coat iron is present in the inside of the seed coat, as no staining was observed when the seed coat was intact or tightly attached to the cotyledons as illustrated in the unstained patch of Fig. 3D and E.

DISCUSSION

The seed coats of mature soybean seeds contain a large percentage of the total seed iron. Our results show that 20% to 40% of the soybean seed iron was found in the seed coat, a tissue that comprises 6% to 8% of the total seed dry weight. These results are similar to previous findings by Tiffin and Chaney [10], but lower seed coat iron concentrations were reported by

Laszlo [11]. It was reported that most of the iron in soybean seed coats was present in the ferrous form, although this speciation was dependent on the genotype and crop year [19]. The presence of ferrous iron in soybeans was also measured by Mössbauer spectrometry, and in this study it was shown that the percentage of ferrous iron is dependent on the developmental stage of the seed [20]. The presence of highly soluble ferrous iron can contribute to dietary iron intake. In agreement, soybean hulls were shown to be an effective iron source in rat assays [21]. In addition, studies using baked soybeans show that they are a good source of nutritional iron [8]. These results altogether indicate the importance of considering the soybean hulls when assessing the nutritional value of soybeans.

Iron and manganese are similarly distributed in soybean radicles. In this study we used micro-PIXE analysis to describe the distribution of iron, zinc, manganese, phosphorus and potassium in soybean seeds (Fig. 1 and 2). Similar analyses have been performed using *A. thaliana* seeds [12]. Iron accumulates similarly in the radicles of *A. thaliana* and of soybean. It was shown that iron accumulated in the provascular bundles of the cotyledons of *A. thaliana* [12] while no accumulation of this element was detected in the soybean cotyledon. Elevated concentration of manganese was observed primarily in the radicle of the soybean seeds (Fig. 1), while it appeared in regions of the cotyledons in *A. thaliana* [12]. Zinc accumulated in the radicle of the soybean seed, mostly near the meristem (Fig. 1), while for *A. thaliana* increased zinc concentration was observed in the provascular tissue of the radicle [12].

Acknowledgments. Technical assistance of Finn Pedersen, Kirsten Sørensen, and Carolina Astudillo. Funding was provided by the Centre for Carbohydrate Recognition and Signalling, the Danish Agency for Science, Technology and Innovation; HarvestPlus; and the Research Foundation of the University of Aarhus, Denmark.

REFERENCES

1. Black RE, Allen LH, Bhutta ZA, Caulfield LE, de Onis M, et al. (2008) Maternal and child undernutrition: global and regional exposures and health consequences. *Lancet* 371: 243–260
2. Meenakshi JV, Johnson N, Manyong VM, De Groote H, Javelosa J, et al. (2007) How cost-effective is biofortification in combating micronutrient malnutrition? An ex-ante assessment. pp. www.harvestplus.org.
3. Nestel P, Bouis HE, Meenakshi JV, Pfeiffer W (2006) Biofortification of staple food crops. *J Nutr* 136: 1064-1067.
4. Stein AJ, Meenakshi JV, Qaim M, Nestel P, Sachdev HP, et al. (2008) Potential impacts of iron biofortification in India. *Soc Sci Med* 66: 1797-1808.
5. Welch RM, Graham RD (2004) Breeding for micronutrients in staple food crops from a human nutrition perspective. *J Exp Bot* 55: 353-364.
6. Welch RM, House WA, Beebe S, Cheng Z (2000) Genetic selection for enhanced bioavailable levels of iron in bean (Phaseolus vulgaris L.) seeds. *J Agr Food Chem* 48: 3576-3580.
7. Broughton WJ, Hernandez GH, Blair M, Beebe S, Gepts P, et al. (2003) Beans (*Phaseolus* spp.)- model food legumes. *Plant Soil* 252: 55.
8. Murray-Kolb LE, Welch R, Theil EC, Beard JL (2003) Women with low iron stores absorb iron from soybeans. *Am J Clin Nutr* 77: 180-184.

9. Ariza-Nieto M, Blair MW, Welch RM, Glahn RP (2007) Screening of iron bioavailability patterns in eight bean (*Phaseolus vulgaris* L.) genotypes using the Caco-2 cell in vitro model. *J Agr Food Chem* 55: 7950-7956.
10. Tiffin LO, Chaney RL (1973) Translocation of iron from soybean cotyledons. *Plant Physiol* 52: 393-396.
11. Laszlo JA (1990) Mineral content in soybean seed coats and embryos during development. *J Plant Nutr* 13: 231.
12. Kim SA, Punshon T, Lanzirotti A, Li L, Alonso JM, et al. (2006) Localization of iron in Arabidopsis seed requires the vacuolar membrane transporter VIT1. *Science* 314: 1295-1298.
13. Prozesky V, Przybylowicz W, Van Achterbergh E, Churms C, Pineda C, et al. (1995) The NAC nuclear microprobe facility. *Nuclear Instruments and Methods in Physics Research B* 104: 36-42.
14. Przybylowicz W, Mesjasz-Przybylowicz J, Pineda C, Churms C, Springhorn K, et al. (1999) Biological applications of the NAC nuclear microprobe. *X Ray Spectrom* 28: 237-243.
15. Przybyłowicz W, Mesjasz-Przybyłowicz J, Migula P, Nakonieczny M, Augustyniak M, et al. (2005) Micro-PIXE in ecophysiology. *X Ray Spectrom* 34: 285-289.
16. Ryan C (2000) Quantitative trace element imaging using PIXE and the nuclear microprobe. *Int J Imag Syst Tech* 11: 219-230.
17. Choi EY, Graham R, Stangoulis J (2007) Semi-quantitative analysis for selecting Fe- and Zn-dense genotypes of staple food crops. *J Food Compos Anal* 20: 496-505.
18. Meguro R, Asano Y, Odagiri S, Li C, Iwatsuki H, et al. (2007) Nonheme-iron histochemistry for light and electron microscopy: a historical, theoretical and technical review. *Arch Histol Cytol* 70: 1-19.
19. Laszlo JA (1988) Content and stability of ferrous iron in soybean hulls. *Cereal Chem* 65: 20-23.
20. Ambe S, Ambe F, Nozaki T (1987) Mossbauer study of iron in soybean seeds. J Agric Food Chem 35: 292-296.
21. Huh MH, Shin MH, Lee YB, Sohn HS (1999) Effect of soybean hull iron on growth, iron bioavailability, and behavioral function in anemic rats induced by iron deficiency during gestation or lactation. *Nutr Res* 19: 1749-1761.